JOURNAL OF BACTERIOLOGY, Aug. 1990, p. 4295–4306
0021-9193/90/084295-12$02.00/0

Vol. 172, No. 8

Correlation between Ultrastructural Differentiation of Bacteroids and Nitrogen Fixation in Alfalfa Nodules

J. VASSE, F. DE BILLY, S. CAMUT, AND G. TRUCHET*

Laboratoire de Biologie Moléculaire des Relations Plantes-Microorganismes, Centre National de la Recherche Scientifique-Institut National de la Recherche Agronomique, B.P. 27, 31326 Castanet-Tolosan Cedex, France

Received 6 February 1990/Accepted 14 May 1990

Bacteroid differentiation was examined in developing and mature alfalfa nodules elicited by wild-type or Fix⁻ mutant strains of *Rhizobium meliloti*. Ultrastructural studies of wild-type nodules distinguished five steps in bacteroid differentiation (types 1 to 5), each being restricted to a well-defined histological region of the nodule. Correlative studies between nodule development, bacteroid differentiation, and acetylene reduction showed that nitrogenase activity was always associated with the differentiation of the distal zone III of the nodule. In this region, the invaded cells were filled with heterogeneous type 4 bacteroids, the cytoplasm of which displayed an alternation of areas enriched with ribosomes or with DNA fibrils. Cytological studies of complementary halves of transversally sectioned mature nodules confirmed that type 4 bacteroids were always observed in the half of the nodule expressing nitrogenase activity, while the presence of type 5 bacteroids could never be correlated with acetylene reduction. Bacteria with a transposon Tn*5* insertion in pSym *fix* genes elicited the development of Fix⁻ nodules in which bacteroids could not develop into the last two ultrastructural types. The use of mutant strains deleted of DNA fragments bearing functional reiterated pSym *fix* genes and complemented with recombinant plasmids, each carrying one of these fragments, strengthened the correlation between the occurrence of type 4 bacteroids and acetylene reduction. A new nomenclature is proposed to distinguish the histological areas in alfalfa nodules which account for and are correlated with the multiple stages of bacteroid development.

Bacteria of the genus *Rhizobium* are able to induce the organogenesis of root nodules on leguminous plants. Nodules are considered organs per se, in which the endosymbiotic bacteria reduce atmospheric nitrogen into ammonia.

The term bacteroid refers to the symbiotic intracellular form of the microsymbiont without regard to size, shape, or location (5). It will be used in this sense in this study. In indeterminate nodules induced by fast-growing rhizobia on temperate legumes (e.g., alfalfa), bacteroids are found in the invaded cells of the central tissue, namely in the infection zone II or early symbiotic zone, and in the nitrogen-fixing zone III or late symbiotic zone (1, 16, 17, 22, 24, 27, 34, 36, 37, 39, 43, 47). These two zones are delimited distally by the bacteria-free meristematic zone I, proximally by the senescent zone IV, and laterally by peripheral tissues such as the nodule parenchyma (i.e., the inner cortex [44]), the vascular bundles, the nodule endodermis, and the outer cortex (36, 44).

Bacteroid development, known as the Bad phenotype (45), has often been described in studies of nodule development in temperate legumes. In alfalfa, bacteroid differentiation has been described in nodules induced by wild-type strains of *Rhizobium meliloti* (16, 17, 27, 35, 43), Fix⁻ mutants (1, 16, 17, 29, 46), and hybrid strains (38, 47) and in wild-type nodules in which senescence was induced by foliar removal (43), by the application of combined nitrogen (23, 35, 37), or by darkness (23). In general, differentiation of wild-type vegetative cells into bacteroids involves an increase in size and pleomorphism, a higher nucleic acid content, and several ultrastructural changes compared with the free-living bacteria. In a previous examination of the ultrastructure and nucleic acid content of alfalfa bacteroids, Paau et al. (24) found that bacteroids active in acetylene reduction were located in the middle region of 6- to 8-week-old nodules and were ultrastructurally "devoid of electron-empty granules and distinct central fibrillar nucleoids." However, in other studies it was shown that, in the late symbiotic zone in which nitrogen fixation is assumed to occur, the cytoplasm of bacteroids was heterogeneous, especially in the proximal part of this zone (16, 17).

The ultrastructural variations of bacteroids during nodule development and the histological location of each ultrastructural type in developing or mature alfalfa nodules are still not well defined. This communication reports on the ultrastructural differentiation of bacteroids in alfalfa nodules induced by the wild-type *R. meliloti* 2011 strain and Fix⁻ mutant derivatives. Our results differentiate five ultrastructural steps in bacteroid development, each restricted to a well-defined histological region of the nodule. The acetylene-reducing capacity of the nodule was correlated with the differentiation of type 4 bacteroids, which are heterogeneous in aspect and which filled the host cells in distal zone III.

MATERIALS AND METHODS

Bacterial strains and plasmids. The bacterial strains and plasmids used in this study are listed in Table 1.

Nodulation assays. Seeds of *Medicago sativa* c.v. Gemini, Iroquois, and Vernal were surface sterilized, germinated, inoculated, and grown in test tubes on nitrogen-free agar slants (39). The wild-type strain *R. meliloti* 2011 was inoculated on several alfalfa cultivars, while mutant strains were tested on *M. sativa* c.v. Gemini only.

Nitrogenase activity. Nitrogenase activity was assayed by the acetylene reduction technique (40). For wild-type associations, the nitrogen-fixing ability was measured on individual whole nodules or nodule sections. Small root segments with attached nodules were excised from the plant between 4 and 42 days after inoculation. Transverse free-hand sec-

* Corresponding author.

TABLE 1. Bacterial strains and plasmids used in this study

Strain or plasmid	Relevant characteristics[a]	Reference
R. meliloti strains		
2011 (SU47)	Wild type, Nod$^+$ Fix$^+$	32
GMI708	2011 derivative, Nod$^+$ Fix$^+$ Rif^r	30
GMI395	Nod$^+$ Fix$^-$, Tn*5* insertion 2.66 in *fixL*	9
GMI347	Nod$^+$ Fix$^-$, Tn*5* insertion 2.3 in *fixJ*	4
GMI5442	Nod$^+$ Fix$^-$, Tn*5* insertion 2.228 in *fixG*	20
GMI394	Nod$^+$ Fix$^-$, Tn*5* insertion 2.64 in *fixG*	20
GMI5443	Nod$^+$ Fix$^-$, Tn*5* insertion 2.247 in *fixG*	20
GMI5441	Nod$^+$ Fix$^-$, Tn*5* insertion 2.222 in *fixH*	20
GMI5455	Nod$^+$ Fix$^-$, Tn*5* insertion 2.416 in *fixI*	20
GMI5459	Nod$^+$ Fix$^-$, Tn*5* insertion 2.405 in *fixI*	20
GMI5453	Nod$^+$ Fix$^-$, Tn*5* insertion 2.451 in *fixI*	20
GMI351	Nod$^+$ Fix$^-$, Tn*5* insertion 2.1 in *fixI*	20
GMI708ΔJB8	Nod$^+$ Fix$^+$, ΔJB8 (Rif^r Bleo^r Nm^r)	30
HG30P2	Nod$^+$ Fix$^+$, ΔHG30P2 (Rif^r Nm^r)	30
HG30P2ΔJB8	Nod$^+$ Fix$^-$, ΔHG30P2ΔJB8 (Rif^r Bleo^r Nm^r)	30
HG30P2 ΔJB8 (pTH2)	Nod$^+$ Fix$^+$ by complementation of reiterated region VI	30
HG30P2 ΔJB8 (pGMI467)	Nod$^+$ Fix$^+$ by complementation of reiterated region VI′	30
Plasmids		
pTH2	pLAFR1 derivative, Tc^r	30
pGMI467	pLAFR1 derivative, Tc^r	30

[a] Rif, Rifampin; Bleo, bleomycin; Nm, neomycin; Tc, tetracycline.

tions were made on 4-week-old nodules under the dissecting microscope proximal to, in the middle of, and distal to the red region of the nodule. Nodule halves were assayed individually for nitrogenase activity immediately after dissection. A sample was identified as Fix$^+$ if acetylene-dependent ethylene production occurred within the 30-min incubation time.

Nitrogenase activity of mutant strains was assayed on the entire nodulated root system of plants collected 3 weeks after inoculation.

Microscopy. Nodules were fixed as described previously (36), dehydrated in an ethanol series, and embedded in Epon. The histological organization of wild-type or mutant nodules was observed on 0.9-μm sections, stained by the basic fuchsin-methylene blue method (18). To locate starch granules, wild-type nodules were fixed with 2.5% glutaraldehyde in 0.15 M sodium cacodylate buffer for 1 h at room temperature, cut into 80-μm longitudinal slices (Microcut H1200; Bio-Rad Laboratories), cleared with sodium hypochlorite for 20 s (36), rinsed with distilled water, stained in a 0.1 M aqueous potassium iodide solution for 20 s, rinsed again, and observed by bright-field microscopy. Ultrastructural differentiation of bacteroids was observed with a Hitachi EM 600 electron microscope on ultrathin sections stained with uranyl acetate and lead citrate (31).

DNA-containing structures were localized at the ultrastructural level by the method of Huxley and Zubay (19). Cell structures known to contain RNA, such as ribosomes, were stained on ultrathin sections of nonosmified nodules as described by Bernhard (6).

RESULTS

Histology of nitrogen-fixing alfalfa nodules. Although several reports have already described the overall histology of effective alfalfa nodules, the organization of such nodules is summarized to serve as a frame of reference. From the distal (apical) part of a nodule to the proximal (basal) region, four central zones can be distinguished (Fig. 1A and B): the bacteria-free meristematic zone I; infection zone II, in which cell differentiation begins; nitrogen-fixing zone III; and senescent zone IV, which usually differentiates 5 weeks after inoculation. With the exception of the apical meristem, the three other zones are surrounded by lateral nodular tissues such as the parenchyma (i.e., the inner cortex [44]), the vascular bundles, and the endodermis. Finally, a cortex surrounds the nodule.

In addition to these tissues, we observed a region located between zone II and zone III which extended over one to three layers of cells (Fig. 1A and B). Light microscopy showed that the invaded host cells of this region were filled with amyloplasts (Fig. 1A and B). While the starch deposition defined a sharp cell-to-cell limit with the distal zone II (Fig. 1A and B), the proximal border of this region was less well defined (Fig. 1B). A drastic reduction in starch accumulation was noticed in the distal cells of the adjacent zone III, which reacted weakly with potassium iodide to reveal small amyloplasts located against the plant cell wall adjacent to the nodule parenchyma (Fig. 1B) or around the intercellular spaces (Fig. 2D). In this paper we will refer to this region as interzone II-III.

Bacteroid differentiation in nitrogen-fixing alfalfa nodules. The first objective of this study was to describe the different steps in bacteroid differentiation and to determine the histological zones of the nodule where each step occurred preferentially or exclusively. The experiments were performed on nitrogen-fixing nodules elicited by *R. meliloti* 2011 on the three alfalfa cultivars examined. The nodules were processed 3, 4, or 5 weeks after inoculation.

Ultrastructural studies showed that five types of bacteroids could be observed successively from distal zone II to proximal zone III of the nodule. For each bacteroid type, nucleoid- and ribosome-enriched regions were identified by differential staining of nucleic acids.

(i) Type 1. The type 1 bacteroid observed in the distal part of zone II corresponded to bacteria recently released from the infection threads (Fig. 2A). These rod-shaped and dividing type 1 bacteroids showed a central nucleoid with condensed DNA fibrils and ribosomes in the periphery of the cytoplasm. A large periplasmic space was observed between slightly convoluted inner and outer membranes, and the peribacteroid membrane appeared irregular in shape due to local fusions with plant cytoplasmic vesicles.

(ii) Type 2. The type 2 bacteroid, which elongated without dividing (Fig. 2B), characterized rhizobia in proximal zone II. Ultrastructurally, type 2 bacteroids had ribosomes either at the periphery of the cytoplasm or as inner patches intermixed with DNA fibrils. Both periplasmic and peribacteroid spaces were reduced, and the peribacteroid membrane was more regular in shape.

The progression of bacteroid differentiation from type 1 to type 2 could be found in the same plant cells of middle zone II. In contrast, only type 2 bacteroids were seen in the proximal cells of this zone.

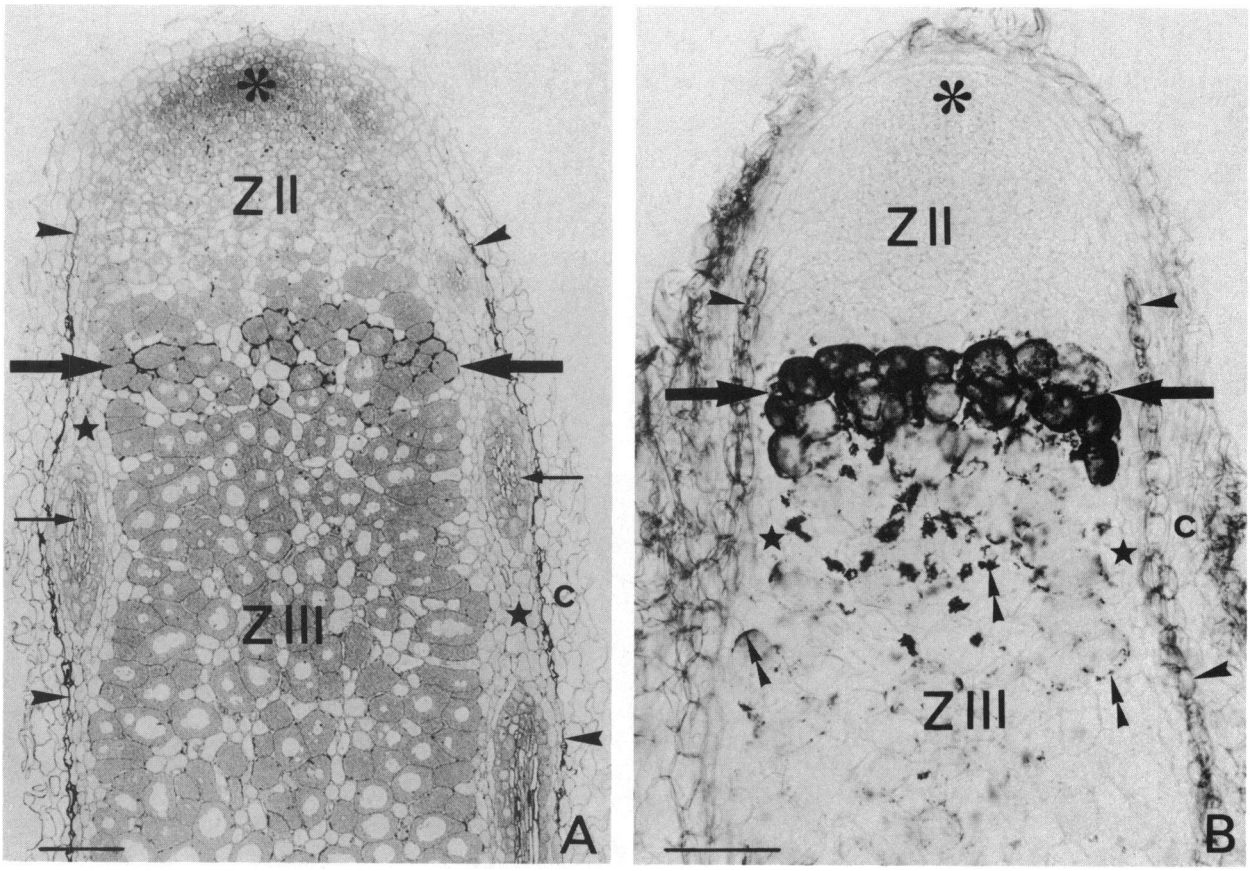

FIG. 1. Histology of 4-week-old wild-type alfalfa nodules (A). Longitudinal semithin section showing the meristematic zone I (asterisk), infection zone II (ZII), interzone II-III (large arrows), and the nitrogen-fixing zone III (ZIII). The nodule parenchyma (stars), the vascular bundles (small arrows), the nodule endodermis (arrowheads), and the nodule cortex (c) are shown. (B) Longitudinal slice (80 μm) cleared with sodium hypochlorite. Amyloplasts are stained with potassium iodide in interzone II-III (large arrows). The double arrowheads point to small amyloplasts in distal zone III. Bars, 100 μm.

(iii) Type 3. The type 3 bacteroid was found exclusively in the amyloplast-rich cells of interzone II-III (Fig. 2C). The transition from the type 2 to the type 3 bacteroid occurred in adjacent cells (Fig. 2C). At this step of differentiation, the bacteroids stopped elongating and displayed cytoplasmic heterogeneity. However, no strict zonation was observed between electron-dense ribosome clusters and electron-translucent areas containing DNA fibrils. The membranes limiting each bacteroid, including the peribacteroid membrane, were smooth, often contacting each other, with small periplasmic and peribacteroid spaces.

Unlike type 2 bacteroids, type 3 bacteroids filled most of the host cells. These cells were characterized by a higher ribosomic density, starch accumulation in the plastids, and confinement of the plant cell organelles against the cell wall.

(iv) Type 4. The type 4 bacteroid was restricted to the distal cells of zone III, which accumulated very little starch in their plastids and stained strongly due to their high content of ribosomes and polysomes (Fig. 2D and E). Type 4 bacteroids were the same size as type 3 bacteroids but showed a marked heterogeneity, with regions of greater electron density enriched with ribosomes and/or polysomes and electron-translucent regions in which DNA fibrils were observed with difficulty (Fig. 2D and E). The boundaries between regions were generally very distinct (Fig. 2D and E).

In nitrogen-fixing nodules with a completely developed zone III, the distal cells were filled with type 4 bacteroids in a volume of tissue spanning 8 to 12 cell layers. This volume did not vary among nodules developing between 3 and 6 weeks after inoculation.

(v) Type 5. The last step in bacteroid differentiation occurred in proximal zone III. Type 5 bacteroids varied in morphology and showed a progressive loss of cytoplasmic heterogeneity. This loss occurred by dispersion of the ribosome-enriched areas. Bacteroids in the final stage of differentiation displayed a homogeneous cytoplasm of faint electron density, with ribosomes and DNA fibrils no longer visible (Fig. 2F). Both bacteroids and host plant cells stained weakly in proximal zone III compared with distal zone III (compare Fig. 2E and F).

Type 5 bacteroids decreased gradually in number during the differentiation of the proximal degenerative zone IV of the nodule. Ghost membranes of plant and bacteroid origin were the ultimate result of the senescing process (not shown).

It is worth mentioning that the ultrastructural characteristics of each bacteroid type were not affected by either the fixative used (glutaraldehyde or a glutaraldehyde-paraformaldehyde mixture with or without further osmification) or the inclusion resin (Epon, Spurr, araldite, L. R. white) (not shown) and that the same sequence of bacteroid differentiation was found in nodules of the three alfalfa cultivars studied.

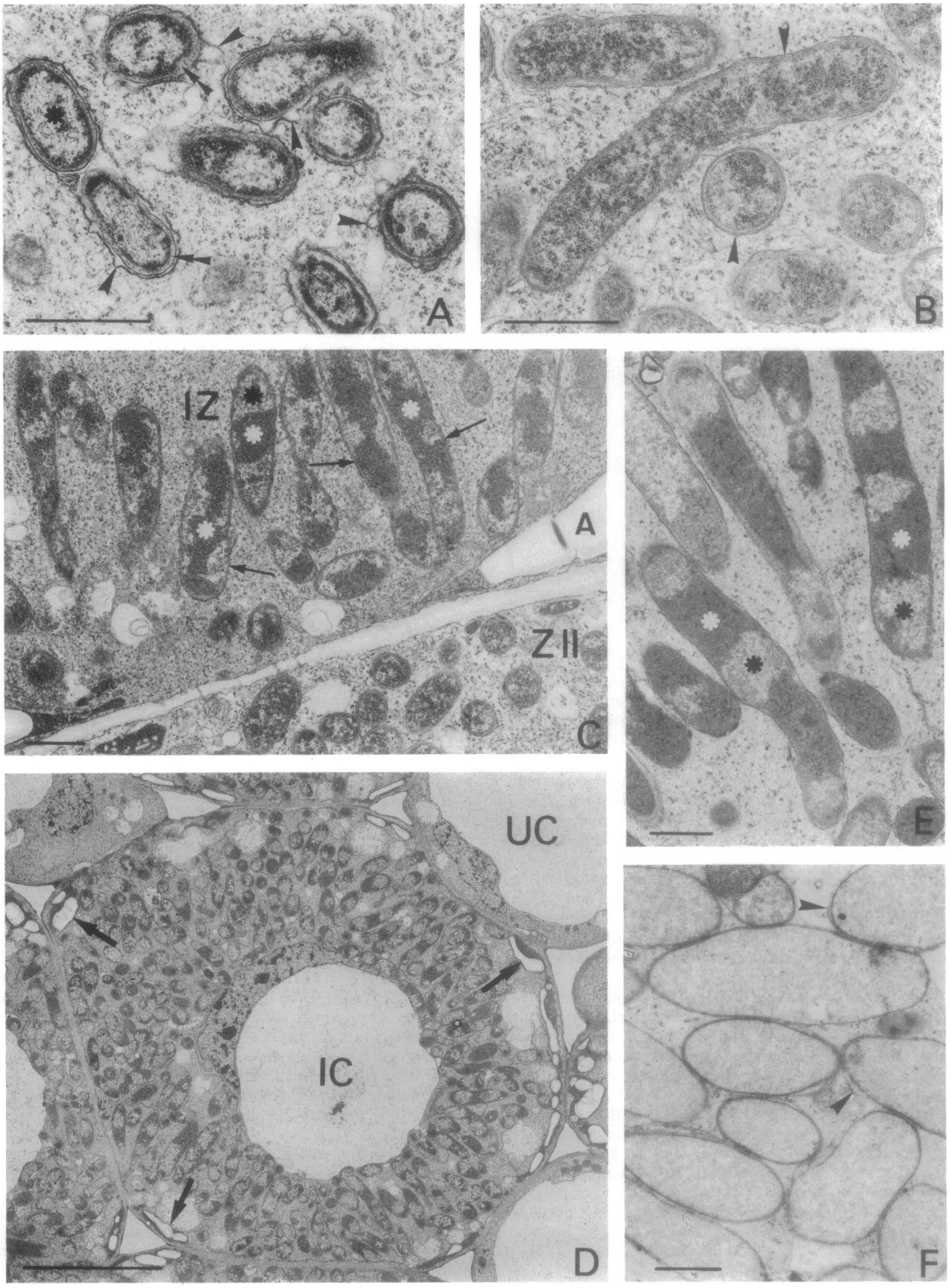
A
B
IZ
A
ZII
C
E
UC
IC
D
F

Correlation between nodule development, bacteroid differentiation, and nitrogen fixation. The second objective of this study was to identify the steps of bacteroid differentiation which were correlated to nitrogen fixation in wild-type *M. sativa* c.v. Gemini nodules. For this purpose, the nitrogen-fixing capacity of both whole individual nodules collected at different ages and transverse sections of 4-week-old nodules was determined. Then, each sample was processed for structural studies by light and electron microscopy.

As a control, we examined whether the nitrogenase activity assay affected the ultrastructure of the plant or the bacteroid cells. Five nodules were incubated for 30 min with acetylene before being processed for microscopy. No histological or ultrastructural differences were noticed between test nodules and controls processed in the same way but incubated in air (not shown).

Developing nonfixing nodules collected from 4 to 8 days after inoculation differed in inner histology, the youngest being only a meristematic area while the oldest showed the establishment of an inner zonation (Fig. 3A and B). According to the age of the developing nodules, type 1 and type 2 bacteroids in zone II or type 3 bacteroids in interzone II-III displayed the same ultrastructural features as described above in the equivalent zones of mature nodules (not shown). The interzone was larger in developing nodules than in mature nodules and could extend over four to six cell layers. The amyloplasts filled both invaded and the uninvaded cells of this interzone (Fig. 3B). No nitrogenase activity was detected in these young nodules containing type 1, type 2, and type 3 bacteroids.

Developing nodules expressed nitrogenase activity within 8 days following inoculation. Ultrastructural examination of these effective nodules showed that type 4 bacteroids had differentiated in the most proximal nodule cells (Fig. 3C and D). These were the earliest cells of zone III which then fully differentiated into distal and proximal parts of mature nodules as described above. Generally, this zone ceased to enlarge in 5-week-old nodules, when senescence zone IV began to develop (not shown).

The above data strongly suggested that type 4 bacteroids were the first ones associated with nitrogen fixation within the nodule. We next addressed the question of whether type 5 bacteroids express nitrogenase activity by studying nodule segments obtained after transverse sectioning.

The distal and proximal parts of 20 nodules collected 4 weeks after inoculation were transversally sectioned, assayed for nitrogenase activity, and individually prepared for microscopy as described in Materials and Methods. We found that for 12 out of the 20 nodules assayed, both complementary halves reduced acetylene. Histological and ultrastructural data showed the presence of type 4 bacteroids in all of the specimens, while type 5 bacteroids were also observed in the proximal parts (not shown). In the eight remaining nodules, acetylene was reduced by the distal halves alone at a mean rate of 501±42 nM after an incubation time of 30 min, but not by the complementary proximal parts. Cytological studies showed once again the presence of type 4 bacteroids in effective specimens, whereas type 5 bacteroids alone were observed in the ineffective proximal parts (not shown). These data confirmed that type 4 bacteroids were active in nitrogen fixation and indicated that the presence of type 5 bacteroids was not correlated with any detectable acetylene reduction in mature alfalfa nodules.

Bacteroid differentiation in alfalfa nodules induced by Fix^+ and Fix^- mutant strains. The last objective of this study was to describe the structure of Fix^- and Fix^+ nodules incited by *R. meliloti* mutant strains and to confirm whether the effectiveness of a nodule was correlated with the differentiation of type 4 bacteroids. The mutants were isogenic derivatives of the parental strain *R. meliloti* GMI708 and were obtained by transposon Tn*5* insertions in or deletions of the *fix* region located 200 kilobases (kb) downstream of the *nifHDK* structural genes in pSym (4, 30) (Fig. 4). The mutants were inoculated on *Medicago sativa* c.v. Gemini, and the nodules were processed for light and electron microscopy 3 or 4 weeks after inoculation.

The symbiotic properties of the parental strain were checked first. This strain induced nitrogen-fixing nodules which displayed the same histology and ultrastructure as described above for nodules induced by the wild-type *R. meliloti* 2011.

The first set of mutant strains carried Tn*5* insertions in *fixL*, *fixJ*, *fixG*, *fixH*, or *fixI* (Fig. 4). All these strains induced Fix^- nodules which exhibited significant ultrastructural deviations from the wild-type nodule. Histologically, the nodules showed a cellular zonation that was reduced to meristematic zone I, infection zone II, and interzone II-III (Fig. 5A). Interzone II-III, which was described above, consisting of cells filled with amyloplasts, appeared much larger than in wild-type nodules and extended from 6 to 10 layers of cells, depending on the strain. In such nodules, no zone III comparable to that described for wild-type nodules was observed, and consequently, senescent zone IV differentiated adjacent to interzone II-III (Fig. 5A).

Electron microscopy studies showed that irrespective of the mutant strain, bacteria were released from infection threads and differentiated into type 1 and type 2 bacteroids in the distal and proximal zone II, respectively. Nevertheless, slight ultrastructural differences emerged between mutant strains with respect to their ability to differentiate into type 3 bacteroids and the occurrence of senescence. Thus, in the earliest-senescing nodules elicited by *fixL*, *fixJ*, and *fixI* mutants, bacteroid differentiation was blocked at the stage of type 2 bacteroids (Fig. 5B). In such nodules, senescent bacteroids, which were characteristically nonelongated, electron dense, and irregularly shaped, were observed concomitantly with differentiated bacteroids in proximal zone II (Fig. 5B). In nodules induced by *fixH* or *fixG* mutants, some but not all bacteria were able to differentiate into type 3 bacteroids (Fig. 5C and D). Senescence of bacteroids occurred either concomitantly with bacteroid differentiation in plant cells filled with amyloplasts (Fig. 5C) or between

FIG. 2. Ultrastructural differentiation of bacteroids in 4-week-old nitrogen-fixing alfalfa nodules. (A) Type 1 bacteroids. (B) Type 2 bacteroids. (C) Cell-to-cell ultrastructural changes from proximal zone II (ZII) to interzone II-III (IZ). Invaded cells of interzone II-III are filled with type 3 bacteroids (arrows). Note the difference in cytoplasm density between the two adjacent plant cells. A, Amyloplasts. (D) Distal zone III. Uninvaded cells (UC) and invaded cells (IC) filled with heterogeneous type 4 bacteroids. The large arrows indicate small amyloplasts located near intercellular spaces. (E) Heterogeneous type 4 bacteroids. (F) Homogeneous type 5 bacteroids. In all micrographs: black asterisks, nucleoids; white asterisks, ribosome-enriched regions of bacteroid cytoplasm; arrowheads, peribacteroid membranes. In panel A, the double arrowheads point to the periplasm. Note polysomes in the host cell cytoplasm in panels B and E. (D) Bar, 10 μm. (A, B, C, E, F) Bars, 1 μm.

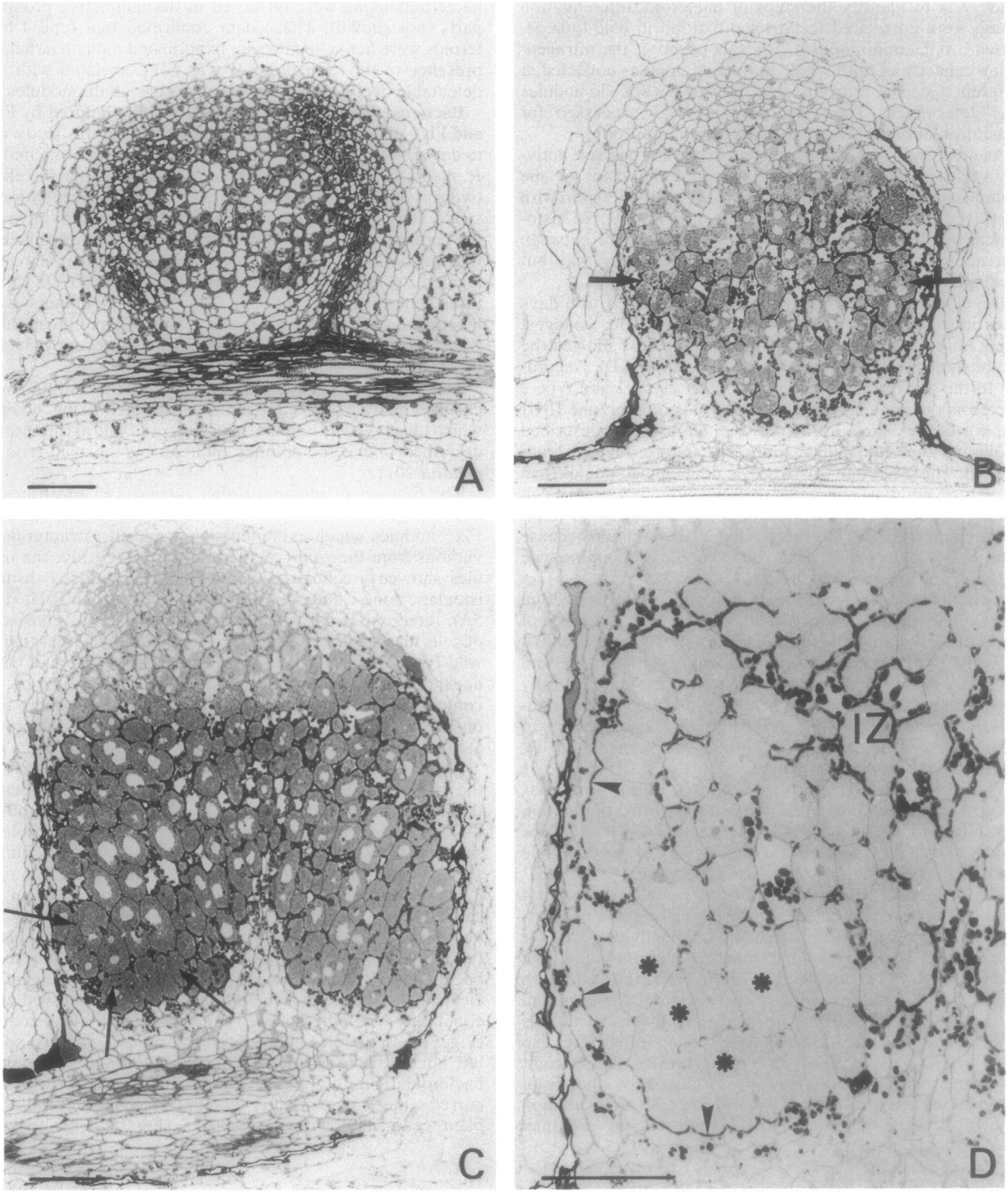

FIG. 3. Histology of developing alfalfa nodules observed by light microscopy. (A and B) Longitudinal sections of inefficient nodules processed 5 days (A) and 7 days (B) after inoculation. Note the histological changes between nodules and the presence of amyloplasts in both invaded and noninvaded cells of the large interzone II-III (arrows) in panel B. (C) Nitrogen-fixing nodule processed 8 days after inoculation. The arrows point to the earliest differentiated host cells of future zone III. (D) Serial section of panel C, stained only with basic fuchsin. Stain emphasizes amyloplasts in interzone II-III (IZ) and against the plant cell wall adjacent to the nodule parenchyma (arrowheads). Amyloplasts are not observed in the cells of differentiating zone III (asterisks). Bars, 100 μm.

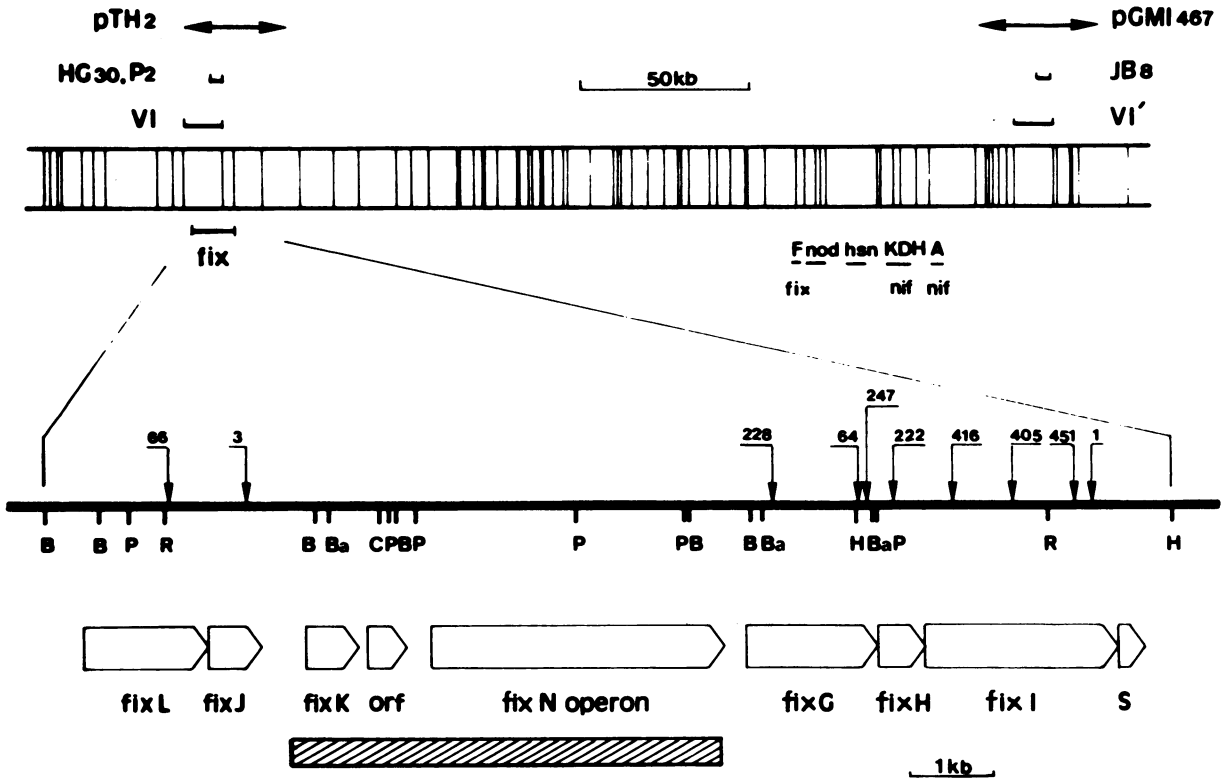

FIG. 4. Partial *Hin*dIII physical map of the *R. meliloti* 2011 plasmid pSym. The deletions in reiterated regions VI and VI' (HG30P2 and JB8, respectively) and the complementary plasmids pTH2 and pGMI467 are shown. Open reading frames and transposon insertions yielding a Fix^- phenotype (thin vertical lines) are indicated above the enlarged physical genetic map of the *fix* region. The hatched box represents the DNA of the *fix* cluster which is reiterated. B, *Bgl*II; Ba, *Bam*HI; C, *Cla*I; H, *Hin*dIII; P, *Pst*I; R, *Eco*RI. This figure is a compilation of data from several sources (3, 4, 20, 30).

adjacent cells in the proximal part of interzone II-III (Fig. 5D). A drastic diminution in starch accumulation in plastids of plant cells which were filled with senescing bacteroids alone was also observed.

Senescing bacteroids showed a characteristic marbled cytoplasm with a pronounced contrast between electron-dense and electron-translucent areas (Fig. 5C and D). These areas were considered remnants of regions which in type 2 and type 3 bacteroids appeared enriched with ribosomes or DNA fibrils, respectively.

Finally, different strains carrying Tn*5* insertions in the same *fix* gene showed the same ultrastructural differentiation.

The second set of mutant strains was modified in reiterated regions of pSym. These regions were region VI, located between the *fixLJ* and *fixGHIS* operons, and its functional copy, region VI', reiterated on the megaplasmid approximately 40 kb upstream of the *nifHDK* structural genes (30) (Fig. 4). The deletion of region VI (*R. meliloti* HG30P2) or VI' (*R. meliloti* GMI708ΔJB8) altered neither the nitrogen-fixing capacity nor the ultrastructure of the nodules, which resembled wild-type nodules (not shown). In contrast, a strain deleted in both regions VI and VI' (*R. meliloti* HG30P2ΔJB8) induced Fix^- nodules (Fig. 6A), which histologically resembled the Fix^- nodules induced by the Tn*5* mutants described above: interzone II-III was enlarged and zone III did not develop. Ultrastructurally, no differentiation beyond type 2 bacteroids in proximal zone II occurred, and a precocious marbled senescence was observed (not shown). These cytological variations disappeared in nodules induced by a doubly-deleted strain complemented with a plasmid bearing one of the reiterated regions [*R. meliloti* $HG30P_2\Delta JB8$(pTH2) and *R. meliloti* $HG30P_2\Delta JB8$ (pGMI467)] (Fig. 4). Such complementations restored the ability of the strains to induce nitrogen-fixing nodules displaying the histology of wild-type nodules (Fig. 6B) and the five ultrastructural types of bacteroids, notably type 4 (Fig. 6C). Thus, the results of the studies with mutants concur with those of the studies with wild-type strains on the strict correlation which exists between the occurrence of type 4 bacteroids and the onset of nitrogen fixation.

DISCUSSION

In mature alfalfa nodules, five successive stages in bacteroid differentiation which differ in both histological location and ultrastructure are observed. The first two types of bacteroids, the dividing type 1 bacteroids and the elongating type 2 bacteroids, are found in infection zone II. The fact that only type 2 bacteroids are observed in proximal zone II indicates that bacterial release which generates type 1 bacteroids is restricted to distal zone II.

Type 3 bacteroids are observed in interzone II-III, which is characterized by starch deposition in the plastids of the invaded cells. Although amyloplasts in cells located proximally to zone II have been described for indeterminate nodules (8), the amyloplast-enriched nodule area had not been identified before as a distinct histological zone. Ultrastructural and molecular results justify this identity. The ultrastructural data presented in this article show that inter-

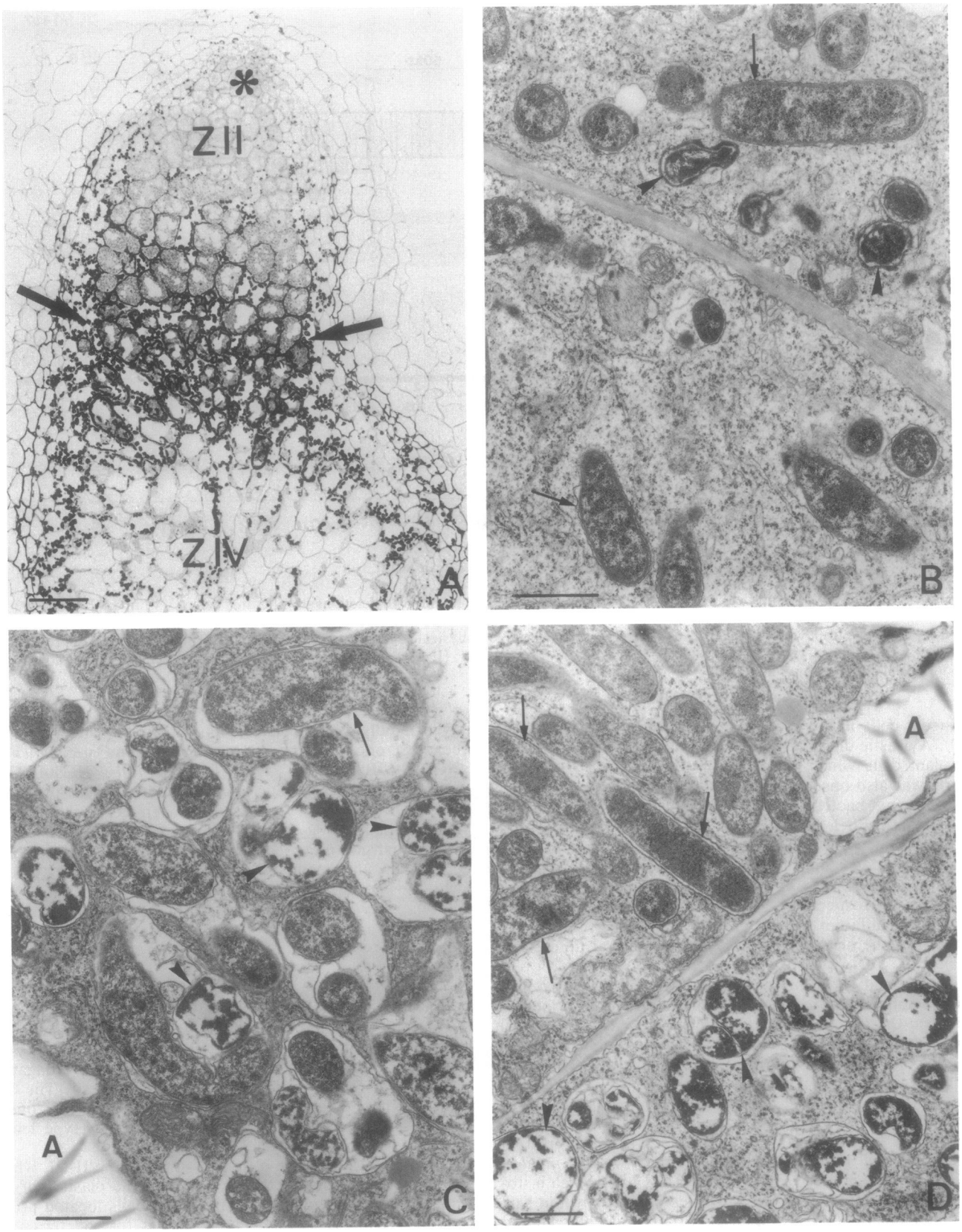

FIG. 5. Histology of a 4-week-old Fix$^-$ alfalfa nodule induced by *R. meliloti* pGMI395 (*fixL*::Tn*5*). Longitudinal section showing the meristematic zone I (asterisk), infection zone II (ZII), large interzone II-III (large arrows), and early senescent zone IV (ZIV). Note the absence of zone III. Bar, 100 μm. (B, C, and D) Ultrastructural differentiation of bacteroids in Fix$^-$ nodules incited by different mutant strains. (B) GMI347, (*fixJ*::Tn*5*). Some bacteroids have differentiated to type 2 (arrows), while others senesced precociously (arrowheads). (C) GMI5441 (*fixH*::Tn*5*). (D) GMI394 (*fixG*::Tn*5*). The arrows point to type 3 bacteroids. Amyloplasts (A) and marbled senescing bacteroids (arrowheads) are seen. (B, C, D) Bars, 1 μm.

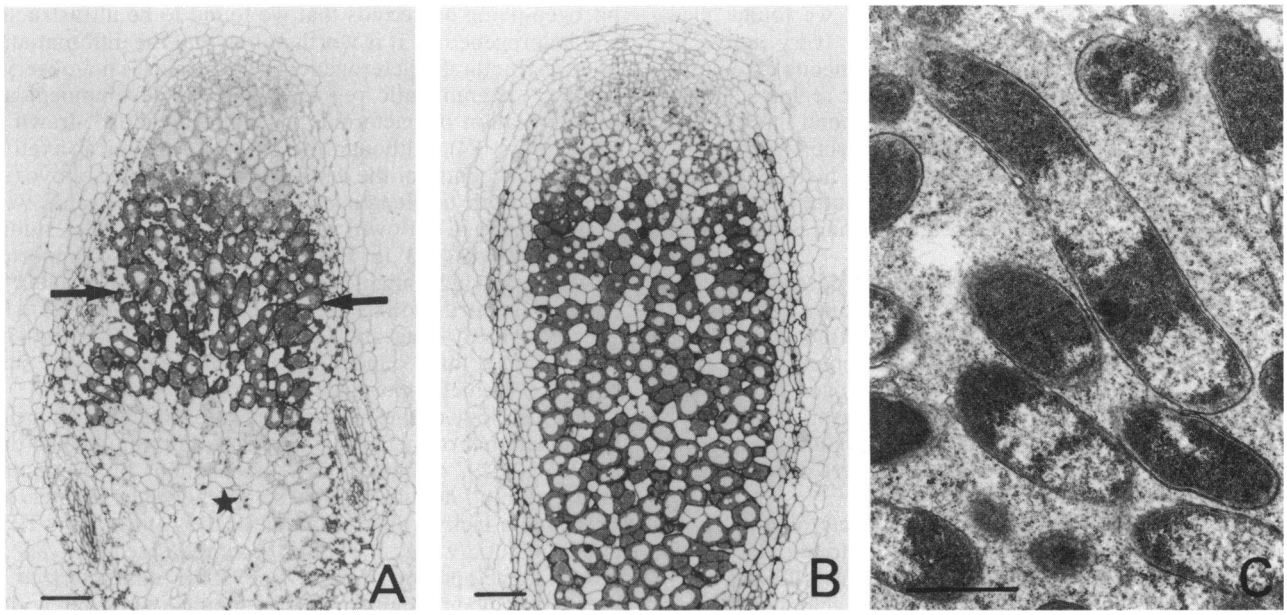

FIG. 6. Histology of 4-week-old alfalfa nodules incited by *R. meliloti* HG30P2ΔJB8 (A) and by *R. meliloti* HG30P2ΔJB8(pTH2) (B). (A) Fix^- nodule. Note the large development of interzone II-III (arrows) adjacent to senescent zone IV (star). (B) Fix^+ nodules after complementation. Restoration of a wild-type nodule histology. In micrographs (A and B) Bars, 100 μm. (C) Ultrastructural differentiation of type 4 bacteroids in Fix^+ nodules incited by *R. meliloti* HG30P2ΔJB8(pGMI467). Bar, 1 μm.

zone II-III constitutes a sharp border corresponding to major changes in the differentiation of both symbionts. Molecular results also show that in correlation with the individualization of interzone II-III, there is a cell-to-cell increase in total RNAs and a cell-to-cell transcription of leghemoglobin genes (D. Barker, F. de Billy, and G. Truchet, unpublished data). Thus, interzone II-III differs fundamentally from the adjacent infection zone II and central zone III.

Type 3 bacteroids display maximal elongation and occupy a greater plant cell volume than bacteroids in the invaded host cells in proximal zone II. This difference in host cell occupancy indicates that bacteroid elongation begins in zone II but is a major feature of differentiation, which ends in interzone II-III. Changes in bacteroid morphology such as elongation and polymorphism are commonly observed in indeterminate nodules (13, 33) and have also been described for free-living rhizobia grown under microaerophilic conditions (2), in soft agar (26), or in liquid medium enriched with succinate (41) or succinate plus mannitol (12). The above results suggest that oxygen concentration and/or organic acids might have a regulatory role in triggering bacteroid differentiation. Although it is not certain that such parameters account for the bacteroid differentiation in alfalfa nodules, it is clear that succinate metabolism is required for this stage in root nodule symbiosis (12).

Cytoplasmic heterogeneity is an important feature which distinguishes the type 3 and type 4 stages of bacteroid differentiation in alfalfa nodules. An increase in DNA content has often been reported during the course of bacteroid differentiation in indeterminate nodules (7, 25, 33). In alfalfa nodules, it is tempting to correlate this increase with the differentiation of type 3 and type 4 bacteroids, in which two or three nucleoid areas per bacteroid are observed.

Previous studies have reported changes in the cytoplasmic heterogeneity of bacteroids in alfalfa nodules (16, 17, 35). For instance, Thornton (34) described "banded" bacteroids in swollen plant cells. These correspond to the type 4 bacteroids which we described ultrastructurally and located histologically in this study. Interestingly, we observed that type 4 bacteroids differentiate in the three *M. sativa* cultivars used in this study. Moreover, we recognized type 4 bacteroids in micrographs published by others studying either wild-type nodules of *M. sativa* c.v. Saranac (27) and *M. sativa* c.v. Agate (43), two alfalfa cultivars that have not been studied in this work, or Fix^+ and some Fix^- nodules elicited by *R. meliloti* mutant strains on *M. sativa* c.v. Iroquois (16). Finally, we found that type 4 bacteroids also differentiate in the nodules of *Melilotus alba* and *Trigonella suavissima*. These results show that the differentiation of type 4 bacteroids is a common feature of nodules of these plant species nodulated by *R. meliloti* strains.

In wild-type alfalfa nodules, type 5 bacteroids are concentrated in proximal zone III. Type 5 bacteroids are observed only if type 4 bacteroids have already differentiated and are not correlated with acetylene reduction. Bacteroids ultrastructurally similar to the type 4 or type 5 bacteroids described in this study have been observed in ineffective alfalfa nodules elicited by *fix* or *nif R. meliloti* mutants (16, 17), although this was in a histological zone different from that in which these bacteroids are usually observed in nitrogen-fixing nodules (interzone II-III versus zone III). Unfortunately, in these studies it was not possible to determine whether the differentiation of type 4 bacteroids preceded further differentiation into type 5.

There are some discrepancies between data concerning the histological location of equally differentiated bacteroids types described in this article and in previous studies. For example, bacteroids displaying the ultrastructural characteristics of type 2 bacteroids, found in this study in the nonfixing zone II, have been described in "the distal portion of the nitrogen-fixing zone (late symbiotic zone)" (16, 17) of alfalfa c.v. Iroquois nodules. Likewise, type 3 bacteroids observed in interzone II-III in this study have been described in "the more proximal part of the late symbiotic

zone" (17), i.e., proximal zone III, which we found filled with type 5 bacteroids. Also, bacteroids "very active in nitrogen fixation" and displaying a homogeneous cytoplasm have been observed in the cells of the middle region of alfalfa c.v. Vernal nodules (22, 24), whereas we found this zone to be infected with heterogeneous type 3 and type 4 bacteroids. We hope that this study, which defines the histological and ultrastructural criteria of bacteroid differentiation, will be useful for further investigations on the fine structure of alfalfa nodules.

The sequence of bacteroid differentiation described in this article differs from that described for clover nodules by Gourret and Fernandez-Arias (14). These authors found that *R. leguminosarum* biovar *trifolii* differentiated through seven steps, with bacteroids in the nitrogen-fixing area displaying no heterogeneity in their cytoplasm and showing a greater polymorphism than in alfalfa nodules, in which relatively few X- or Y-shaped bacteroids were observed (35; this work).

Our study indicates that only type 4 bacteroids in distal zone III can reduce acetylene, while the four other types represent non-nitrogen-fixing bacteroids. The following lines of evidence support such conclusions: (i) developing but still inefficient wild-type nodules, have types 1, 2, and 3 but lack type 4 bacteroids; (ii) type 4 bacteroids are observed only in developing nodules or in nodule segments expressing nitrogenase activity; (iii) in proximal nodule segments which do not reduce acetylene, host cells in zone III are filled exclusively with type 5 bacteroids; and (iv) comparison of Fix^- and Fix^+ strains confirmed the correlation between the differentiation of type 4 bacteroids and the onset of nitrogen fixation. However, it should be emphasized that the micrographs published by Hirsch et al. (16, 17) show that bacteroids displaying ultrastructural features of type 4 and/or type 5 bacteroids as described in this work also differentiate in amyloplast-filled cells of Fix^- alfalfa nodules incited by *nif* and *fix R. meliloti* mutant strains. Considered together, the results from both Hirsch and colleagues (16, 17) and our own laboratory lead to the following conclusions. (i) In alfalfa, the five bacteroid types may differentiate irrespective of the nitrogen-fixing ability of the nodule. (ii) The differentiation of bacteroids into type 4 is necessary but not sufficient to allow the expression of nitrogenase activity by the endosymbiotic bacteria. (iii) The presence of type 5 bacteroids is indicative of a nodule which is or has been active in nitrogen fixation, unless found in nodule cells filled with amyloplasts.

To our knowledge, only Paau et al. (24) have attempted to define the ultrastructural features of bacteroids active in nitrogen fixation. There are discrepancies between our results and those of Paau et al. (24), who reported that bacteroids which were very active in acetylene reduction were observed in the "middle region" of the nodule and were ultrastructurally "devoid of electron-empty granules and distinct central fibrillar nucleoids." In this study we have shown that five bacteroid types are observed in three different histological zones and that the nitrogen-fixing area is histologically and ultrastructurally well defined. Thus, identifying the "middle region" of a nodule as the nitrogen-fixing region without defining its distal and proximal borders is inadequate, and ascertaining that only one bacteroid type is observed in such a "middle region" is misleading. It is likely that the bacteroids claimed as nitrogen-fixing by Paau et al. (24) were located in the proximal part of the "middle region" of nodules. In such a case, the illustrated bacteroids would correspond to the nonfixing type 5 bacteroids described in this work in proximal zone III rather than to the nitrogen-fixing bacteroids that we found to be ultrastructurally heterogeneous. It is worth noting that the differentiation of ultrastructurally heterogeneous bacteroids is not observed on the "diagrammatic representation of development and transformation of bacteroids in alfalfa nodules" drawn by the authors (24). Although the nature of chemical fixatives could not account for the discrepancies discussed above (see Results), both the length of fixation (24 h in Paau's work versus 90 min in our own) and the age of the nodules studied (6 to 8 weeks old in Paau's work) are also important parameters which might lead to controversial results. Finally, it is worth noting that our results demonstrate what was remarkably suggested, 60 years ago, by Thornton (34), who assumed that "banded rods were presumably the stage which is of chief importance in nitrogen fixation."

The histology of the Fix^- nodules described in this article resembles that of ineffective alfalfa nodules studied to date (1, 16, 17, 29, 42, 46). Thus, independent of the mutant strain, all Fix^- nodules studied so far show a large interzone II-III and a lack of differentiation of the central zone III or late symbiotic zone. It should be emphasized that an extended development of interzone II-III characterizes an ineffective nodule, either a developing wild-type nodule which does not yet express nitrogenase activity or a Fix^- mature nodule. The causal relationship between the two events is still not understood. In this study, differences between Fix^- nodules have been observed regarding bacteroid ultrastructure, and the mutant strains have been classified into two groups according to the step at which the differentiation of bacteroids is blocked. From our data and the examination of micrographs published by colleagues, it appears that the differentiation of an *R. meliloti nifA*::Tn*5* mutant (strain 1354) is also stopped at type 2 (17), while many *fix* and *nif* mutants of *R. meliloti* (16, 17; this study) are unable to differentiate beyond type 3. This was also the ultimate step in bacteroid differentiation observed in nodules incited by wild-type *R. meliloti* strains on an ineffective genotype of *M. sativa* c.v. Saranac (42). It has been mentioned in this discussion that bacteroids which are ultrastructurally similar to type 4 and type 5 bacteroids are also observed in Fix^- alfalfa nodules (16, 17). The ultrastructural data showing that mutations in bacterial genes impair the differentiation of bacteroids do not lead to the conclusion that the mutated genes are directly controlling bacteroid differentiation. A block in differentiation might be the consequence of an epistatic effect of the Fix^- phenotype of the elicited nodules.

Legume-*Rhizobium* interactions involve a series of plant-bacterium signals which activate the successive steps in nodulation (10, 11, 15, 21, 28, 39). In this study, it is shown that one of these steps, nitrogen fixation, is restricted to a short nodule area made up of a relatively constant number of plant cell layers filled with type 4 bacteroids.

To account for such an active area, we suggest a modification of the terminology of the nodule zones as follows. We propose to call the zone previously termed infection and differentiation zone II or the early symbiotic zone "prefixing zone II." This term would identify the nodule area inactive in nitrogen fixation, in which differentiation of both symbionts begins and continues progressively. As there is currently no term for the non-nitrogen-fixing amyloplast-enriched part of efficient alfalfa nodules, we suggest the term "interzone II-III" used in this study. In this area, symbionts display ultrastructural and molecular changes in a cell-to-cell fashion. Finally, we propose to subdivide nitrogen-fixing zone III or late symbiotic zone into "nitrogen-fixing zone

III" in the distal location and "ineffective zone III," restricted to the proximal host cells which no longer express nitrogenase activity. Cytological changes from the distal to the proximal part occur progressively all along zone III. As used previously, the terms meristematic zone I and senescent zone IV should be maintained to qualify, respectively, the apical meristem and the most proximal zone of mature nodules where both symbionts degenerate.

In conclusion, this work documents the ultrastructure of bacteroid differentiation in alfalfa nodules and identifies the nitrogen-fixing form of intracellular rhizobia. This study should be useful for further investigations devoted to the cellular location of plant or bacterial gene expression during alfalfa nodule ontogenesis.

ACKNOWLEDGMENTS

We thank Frank Dazzo and colleagues from this laboratory for helpful discussions and valuable criticism, Anne Stanford and Dan Brown for reviewing the English, Corinne Bertin for typing the manuscript, and René Odorico for drawing Fig. 4.

LITERATURE CITED

1. **Aguilar, O. M., D. Kapp, and A. Pühler.** 1985. Characterization of a *Rhizobium meliloti* fixation gene (*fixF*) located near the common nodulation region. J. Bacteriol. **164**:245–254.
2. **Avissar, Y., and R. Gollop.** 1982. Bacteroid characteristics in microaerophilic *Rhizobium*. Isr. J. Bot. **31**:112–118.
3. **Batut, J., M. L. Daveran-Migot, M. David, J. Jacobs, A. M. Garnerone, and D. Kahn.** 1989. *fixK*, a gene homologous with *fnr* and *crp* from *Escherichia coli*, regulates nitrogen fixation genes both positively and negatively in *Rhizobium meliloti*. EMBO J. **8**:1279–1286.
4. **Batut, J., B. Terzaghi, M. Ghérardi, M. Huguet, E. Terzaghi, A. M. Garnerone, P. Boistard, and T. Huguet.** 1985. Localization of a symbiotic *fix* region on *Rhizobium meliloti* pSym megaplasmid more than 200 kilobases from the *nod-nif* region. Mol. Gen. Genet. **199**:232–239.
5. **Bergersen, F. J.** 1974. Formation and function of bacteroids, p. 476–498. *In* A. Quispel (ed.), The biology of nitrogen fixation. North-Holland Publishing Company, Amsterdam.
6. **Bernhard, W.** 1969. A new staining procedure for electron microscopical cytology. J. Ultrastruct. Res. **27**:250–265.
7. **Bisseling, T., R. C. van den Bos, A. van Kammen, M. van der Ploeg, P. van Duijn, and A. Houwers.** 1977. Cytofluorometrical determination of the DNA contents of bacteroids and corresponding broth cultured *Rhizobium* bacteria. J. Gen. Microbiol. **101**:79–84.
8. **Dart, P. J.** 1975. Legume root nodule initiation and development, p. 468–506. *In* J. G. Torrey and D. T. Clarkson (ed.), The development and fuction of roots. Academic Press, Inc., New York.
9. **David, M., M. H. Daveran, J. Batut, A. Dedieu, O. Dommergue, J. Ghai, C. Hertig, P. Boistard, and D. Kahn.** 1988. Cascade regulation of *nif* gene expression in *Rhizobium meliloti*. Cell **54**:671–683.
10. **Faucher, C., S. Camut, J. Dénarié, and G. Truchet.** 1989. The *nodH* and *nodQ* host range genes of *Rhizobium meliloti* behave as avirulence genes in *R. leguminosarum* bv. *viciae* and determine changes in the production of plant-specific extracellular signals. Mol. Plant-Microbe Interact. **2**:291–300.
11. **Faucher, C., F. Maillet, J. Vasse, C. Rosenberg, A. A. N. van Brussel, G. Truchet, and J. Dénarié.** 1988. *Rhizobium meliloti* host range *nodH* gene determines production of an alfalfa-specific extracellular signal. J. Bacteriol. **170**:5489–5499.
12. **Gardiol, A. E., G. L. Truchet, and F. B. Dazzo.** 1987. Requirement of succinate dehydrogenase activity for symbiotic bacteroid differentiation of *Rhizobium meliloti* in alfalfa nodules. Appl. Environ. Microbiol. **53**:1947–1950.
13. **Goodchild, D. J.** 1978. The ultrastructure of root nodules in relation to nitrogen fixation. Int. Rev. Cytol. Suppl. **6**:235–288.
14. **Gourret, J. P., and H. Fernandez-Arias.** 1974. Étude ultrastructurale et cytochimique de la différenciation des bactéroïdes de *Rhizobium trifolii* Dangeard dans les nodules de *Trifolium repens* L. Can. J. Microbiol. **20**:1169–1181.
15. **Halverson, L. J., and G. Stacey.** 1986. Signal exchange in plant-microbe interactions. Microbiol. Rev. **50**:193–225.
16. **Hirsch, A. M., M. Bang, and F. M. Ausubel.** 1983. Ultrastructural analysis of ineffective alfalfa nodules formed by *nif*::Tn*5* mutants of *Rhizobium meliloti*. J. Bacteriol. **155**:367–380.
17. **Hirsch, A. M., and C. A. Smith.** 1987. Effects of *Rhizobium meliloti nif* and *fix* mutants on alfalfa root nodule development. J. Bacteriol. **169**:1137–1146.
18. **Huber, J. D., F. Parker, and G. F. Odland.** 1968. A basic fuchsin and alkanized methylene blue rapid stain for epoxy embedded tissue. Stain Technol. **43**:83–87.
19. **Huxley, H. E., and G. Zubay.** 1961. Preferential staining of nucleic acid-containing structures for electron microscopy. J. Biochem. Biophys. Cytol. **11**:273–296.
20. **Kahn, D., M. David, O. Dommergue, M. H. Daveran, J. Ghai, P. Hirsch, and J. Batut.** 1989. *Rhizobium meliloti fixGHI* sequence predicts involvement of a specific cation pump in symbiotic nitrogen fixation. J. Bacteriol. **171**:929–939.
21. **Lerouge, P., P. Roche, C. Faucher, F. Maillet, G. Truchet, J. C. Promé, and J. Dénarié.** 1990. Symbiotic host-specificity of *Rhizobium meliloti* is determined by a sulphated and acylated glucosamine oligosaccharide signal. Nature (London) **344**:781–784.
22. **Paau, A. S., C. B. Bloch, and W. J. Brill.** 1980. Developmental fate of *Rhizobium meliloti* bacteroids in alfalfa nodules. J. Bacteriol. **143**:1480–1490.
23. **Paau, A. S., and J. R. Cowles.** 1979. Effect of induced nodule senescence on parameters related to dinitrogen fixation, bacteroid size and nucleic acid content. J. Gen. Microbiol. **111**: 101–107.
24. **Paau, A. S., J. R. Cowles, and D. Raveed.** 1978. Development of bacteroids in alfalfa (*Medicago sativa*) nodules. Plant Physiol. **62**:526–530.
25. **Paau, A. S., D. Lee, and J. R. Cowles.** 1977. Comparison of nucleic acid content in populations of free-living and symbiotic *Rhizobium meliloti* by flow microfluorometry. J. Bacteriol. **129**:1156–1158.
26. **Pankhurst, C. E., and A. S. Craig.** 1978. Effect of oxygen concentration, temperature and combined nitrogen on the morphology and nitrogenase activity of *Rhizobium* sp. strain 32H1 in agar culture. J. Gen. Microbiol. **106**:207–219.
27. **Patel, J. J., and A. F. Yang.** 1981. Light and electron microscopic studies of nodule structure of alfalfa. Can. J. Microbiol. **27**:36–43.
28. **Peters, N. K., J. W. Frost, and S. R. Long.** 1986. A plant flavone, luteolin, induces expression of *Rhizobium meliloti* nodulation genes. Science **233**:977–980.
29. **Putnoky, P., E. Grosskopf, D. T. Cam Ha, G. B. Kiss, and A. Kondorosi.** 1988. *Rhizobium fix* genes mediate at least two communication steps in symbiotic nodule development. J. Cell Biol. **106**:597–607.
30. **Renalier, M. H., J. Batut, J. Ghai, B. Terzaghi, M. Ghérardi, M. David, A. M. Garnerone, J. Vasse, G. Truchet, T. Huguet, and P. Boistard.** 1987. A new symbiotic cluster on the pSym megaplasmid of *Rhizobium meliloti* 2011 carries a functional *fix* gene repeat and a *nod* locus. J. Bacteriol. **169**:2231–2238.
31. **Reynolds, E. S.** 1963. The use of lead citrate at high pH as an electron opaque stain in electron microscopy. J. Cell Biol. **17**:208–213.
32. **Rosenberg, C., P. Boistard, J. Dénarié, and F. Casse-Delbart.** 1981. Genes controlling early and late functions in symbiosis are located on a megaplasmid in *Rhizobium meliloti*. Mol. Gen. Genet. **184**:326–333.
33. **Sutton, W. D., C. E. Pankhurst, and A. S. Craig.** 1981. The *Rhizobium* bacteroid state, p. 149–177. *In* K. L. Giles and A. G. Atherly (ed.), Biology of the *Rhizobiaceae* (Int. Rev. Cytol. Suppl. 13). Academic Press, Inc., New York.
34. **Thornton, H. G.** 1930. The early development of the root nodule of lucerne (*Medicago sativa*, L.). Ann. Bot. **44**:385–392.
35. **Thornton, H. G., and J. E. Rudorf.** 1936. The abnormal struc-

ture induced in nodules on lucerne (*Medicago sativa* L.) by the supply of sodium nitrate to the host plant. Proc. R. Soc. B **120**:240–252.

36. **Truchet, G., S. Camut, F. de Billy, R. Odorico, and J. Vasse.** 1989. The *Rhizobium*-legume symbiosis: two methods to discriminate between nodules and other root-derived structures. Protoplasma **149**:82–88.
37. **Truchet, G. L., and F. B. Dazzo.** 1982. Morphogenesis of lucerne root nodules incited by *Rhizobium meliloti* in the presence of combined nitrogen. Planta **154**:352–360.
38. **Truchet, G., F. Debellé, J. Vasse, B. Terzaghi, A. M. Garnerone, C. Rosenberg, J. Batut, F. Maillet, and J. Dénarié.** 1985. Identification of a *Rhizobium meliloti* pSym 2011 region controlling the host specificity of root hair curling and nodulation. J. Bacteriol. **164**:1200–1210.
39. **Truchet, G., M. Michel, and J. Dénarié.** 1980. Sequential analysis of the organogenesis of lucerne (*Medicago sativa*) root nodules using symbiotically defective mutants of *Rhizobium meliloti*. Differentiation **16**:163–172.
40. **Turner, G. L., and A. H. Gibson.** 1980. Measurement of nitrogen fixation by indirect means, p. 111–138. *In* F. J. Bergersen (ed.), Methods for evaluating biological nitrogen fixation. Wiley, Chichester.
41. **Urban, J. E., and F. B. Dazzo.** 1982. Succinate-induced morphology of *Rhizobium trifolii* 0403 resembles that of bacteroids in clover nodules. Appl. Environ. Microbiol. **44**:219–226.
42. **Vance, C. E., and L. E. B. Johnson.** 1983. Plant determined ineffective nodules in alfalfa (*Medicago sativa*): structural and biochemical comparisons. Can. J. Bot. **61**:93–106.
43. **Vance, C. E., L. E. B. Johnson, A. M. Halvorsen, G. H. Heichel, and D. K. Barnes.** 1980. Histological and ultrastructural observations of *Medicago sativa* root nodule senescence after foliage removal. Can. J. Bot. **58**:295–309.
44. **Van de Wiel, C., B. Scheres, H. Franssen, M. J. van Lierop, A. van Lammeren, A. van Kammen, and T. Bisseling.** 1990. The early nodulin transcript ENOD2 is located in the nodule-specific parenchyma (inner cortex) of pea and soybean root nodules. EMBO J. **9**:1–7.
45. **Vincent, J. M.** 1980. Factors controlling the legume-*Rhizobium* symbiosis, p. 103–109. *In* W. E. Newton and W. H. Orme-Johnson (ed.), Nitrogen fixation, vol II. University Park Press, Baltimore.
46. **Virts, E. L., J. W. Stanfield, D. R. Helinski, and G. S. Ditta.** 1988. Common regulatory elements control symbiotic and microaerobic induction of *nifA* in *Rhizobium meliloti*. Proc. Natl. Acad. Sci. USA **85**:3062–3065.
47. **Wong, C. H., C. E. Pankhurst, A. Kondorosi, and W. J. Broughton.** 1983. Morphology of root nodules and nodule-like structures formed by *Rhizobium* and *Agrobacterium* strains containing a *Rhizobium meliloti* megaplasmid. J. Cell Biol. **97**:787–794.